Second harmonic generation in amorphous silicon-on-silica metamaterial

Jie Xu, Eric Plum, Vassili Savinov, and Nikolay I. Zheludev

View Online   Export Citation   CrossMark

APL Photonics
Become a member of the
Early Career Advisory Board

Find out how

Second harmonic generation in amorphous silicon-on-silica metamaterial

View Online   Export Citation   CrossMark

Jie Xu,[1] [ID]   Eric Plum,[1,a)] [ID]   Vassili Savinov,[1] [ID]   and Nikolay I. Zheludev[1,2] [ID]

AFFILIATIONS

[1] Optoelectronics Research Centre and Centre for Photonic Metamaterials, University of Southampton, Southampton SO17 1BJ, United Kingdom
[2] Centre for Disruptive Photonic Technologies, SPMS, TPI, Nanyang Technological University, Singapore 637371, Singapore

[a)] Author to whom correspondence should be addressed: erp@orc.soton.ac.uk

ABSTRACT

We demonstrate second harmonic generation by using an amorphous silicon metamaterial fabricated on the tip of an optical fiber that collects the generated light. The metamaterial is a double-chevron array that supports a closed-mode resonance for the fundamental wavelength at 1510 nm with a quality factor of 30. The normalized resonant second harmonic conversion efficiency calculated per intensity and square of interaction length is $\sim 10^{-11}$ W^{-1}, which exceeds the previously achieved value for a silicon metamaterial by two orders of magnitude.

I. INTRODUCTION

Second-order nonlinear optical processes are of considerable importance for laser technologies, quantum optics, material characterization, spectroscopy, and imaging. Over the last decade, a substantial effort has been focused on developing plasmonic[1–8] and dielectric[9–12] metamaterials[13] with large nonlinearities for second harmonic generation (SHG). In particular, in silicon-based photonics, second-order optical nonlinearities are required in various information processing schemes.[14,15] In silicon, second-order optical nonlinearity can be imposed by strain, electric field, and interfaces and has been observed in waveguides,[16–22] nanoparticles,[23] nanowires,[24,25] nanopillars,[26] photonic crystal nanocavities,[27] metamaterials,[28–30] and multi-material stacks with silicon.[31,32] Silicon metasurfaces have also been used to enhance the nonlinear response of materials with strong natural second-order nonlinearity.[33,34] Here, we report a fiber-integrated metamaterial manufactured from amorphous silicon that achieves two orders of magnitude higher normalized conversion efficiency than previous silicon metamaterial.[28]

II. SILICON METAMATERIAL ON A FIBER TIP

The all-dielectric metamaterial reported here supports a resonant response at wavelength $\lambda_0 = 1.5$ μm. It is an array of chevron groove pairs, with unit cell dimensions of 1.1×1.0 μm^2, milled into the core of a silica fiber and subsequently coated with a 90-nm-thick amorphous silicon layer; see Fig. 1. The metamaterial geometry was chosen by considering that SHG normal to a two-dimensional structure—that is pumped at normal incidence—is permitted for structures with either threefold or absent rotational symmetry,[35,36] while resonant enhancement of SHG may be expected from Fano resonances that occur in pairs of slightly different resonators.[37] A chevron—two identical lines forming an angle—is arguably the simplest structure lacking rotational symmetry. Chevrons can be easily fabricated and combined into a compact unit cell that is smaller than its resonant wavelength. The point symmetry group of the metamaterial is D$_1$ [see Figs. 1(b) and 1(c)], limiting the allowed components of the second-order nonlinear susceptibility tensor to $\chi^{(2)}_{yyy}$, $\chi^{(2)}_{yxx}$, and $\chi^{(2)}_{xxy} = \chi^{(2)}_{xyx}$, where the first index indicates the polarization of the second harmonic photon and the other indices indicate the polarizations of the pump photons.

Within the double-V unit cell, the V-elements have different sizes for the structure to support an anti-symmetric Fano-type closed mode at 1.5 μm wavelength [Fig. 1(d)] coupled to free-space radiation with linear polarization oriented along its symmetry axis[37–40] [y axis in Fig. 1(c)]. The metamaterial has been manufactured on the tip of a cleaved silica optical fiber (Thorlabs SM980-5.8-125, single mode at pump wavelengths) that collects and guides light
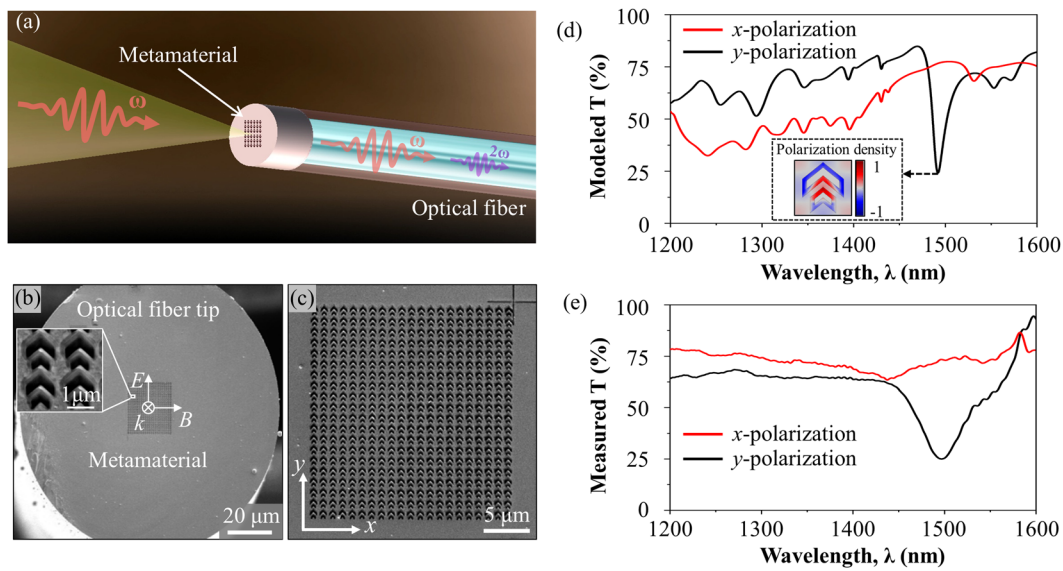
FIG. 1. Nonlinear silicon metamaterial on a fiber tip. (a) Artistic impression of the experimental characterization of the metamaterial's nonlinearity. (b) SEM image of the nonlinear metamaterial fabricated on the end-facet of a single-mode optical fiber. The metamaterial covers the core of the cleaved optical fiber and consists of pairs of chevron grooves in silica, coated with an amorphous silicon layer. Inset: a magnified view of a metamaterial section. (c) Magnified view of the entire metamaterial. (To prevent charging, SEM imaging took place with an additional gold coating that was subsequently removed.) (d) Modeled and (e) measured linear transmission spectra of the metamaterial as a function of wavelength for x (red) and y (black) polarization. The inset in (d) shows the y component of the linear polarization density distribution at the resonance.

transmitted or radiated by the metamaterial; see Figs. 1(a) and 1(b). The fiber's numerical aperture of 0.13 implies that only the 0th-order diffraction of generated second harmonic radiation will be collected. During fabrication, to reduce gallium deposits,[40] the fiber tip is first coated with a thin layer of gold, and then, the V-shaped grooves are created by milling with a focused gallium ion beam through the gold layer to the depth of about 256 nm into silica. After removing the sacrificial gold layer, a 90-nm layer of amorphous silicon is deposited by plasma enhanced chemical vapor deposition on the entire patterned fiber tip. The metamaterial covers the entire core of the fiber, which has a nominal diameter of 10 μm. The metamaterial's thickness, from the lowest point of the silicon layer at the bottom of the chevron grooves to its highest point at the silicon/air interface in between the chevron pairs, is L = 346 nm.

The metamaterial's transmission spectra were modeled (Comsol Multiphysics 5.4) assuming a plane wave normally incident onto a unit cell with periodic boundary conditions, Fig. 1(d). The simulations assume a real refractive index of 1.44 for glass and the complex refractive index of the silicon layer according to ellipsometry measurements on an unstructured area (supplementary material, Fig. S1). The transmission spectra of the structure were measured by illuminating the fiber tip with normally incident linearly polarized white light and detecting the transmitted light with an optical spectrum analyzer (Ando AQ-6315E), using an unstructured cleaved fiber without the silicon film as a reference, Fig. 1(e). Experimental and modeled transmission spectra of the metamaterial are in qualitative agreement. The closed-mode resonance is seen at a wavelength of 1.5 μm, only under y-polarized illumination [along the symmetry axis; see Fig. 1(c)]. According to our simulations, the

electric field at the silicon interfaces is up to 8× larger than the incident field (supplementary material, Fig. S2). The experimentally observed quality factor of this resonance is about 30, calculated by $Q = \lambda_0/\Delta\lambda$, where λ_0 = 1.5 μm is the resonance's central wavelength and $\Delta\lambda$ is the resonance's full width at half maximum (FWHM). Compared with the modeling, the measured resonance is wider due to fabrication-related residual contamination with gallium and inhomogeneous broadening (i.e., slight variations in sizes of key features across different unit cells).

III. SECOND HARMONIC GENERATION

Considering that second harmonic generation by unstructured interfaces vanishes at normal incidence[41] and in order to detect SHG caused by the metamaterial structure, we measure SHG with a normally incident pump beam, which also ensures that 0th order SHG diffraction is within the acceptance angle of the optical fiber. The second harmonic response of the metamaterial was characterized in the pump wavelength range from 1440 to 1610 nm with linearly polarized 200 fs optical pulses of up to 35 mW average power (~9 GW/cm^2 peak intensity) and an 80 MHz repetition rate from an optical parametric oscillator (Spectra Physics Inspire HF 100). Transmitted pump light was filtered out. As control experiments, the same nonlinear measurements were conducted with a bare fiber tip and on a tip of fiber covered by an unstructured 90-nm-thick layer of CVD-silicon. Strong second harmonic emission is observed only for y-polarized pump light at 1510 nm wavelength with the metamaterial-bearing fiber [Fig. 2(a)], while control experiments detected no
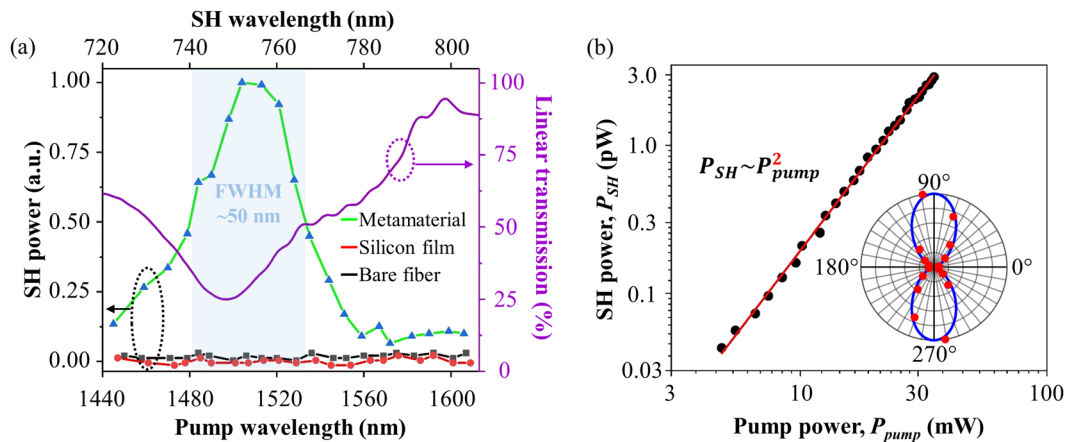
FIG. 2. Observation of second harmonic generation. (a) Detected spectral dependence of second harmonic (SH) emission by a metamaterial on a cleaved fiber (green), an unstructured silicon film on a cleaved fiber (red), and an unstructured bare cleaved fiber (black) alongside the metamaterial's linear transmission spectrum (purple) for y-polarized pump light. (b) Power dependence of second harmonic generation by the metamaterial (black dots) with a quadratic fit (red curve) at 1510 nm pump wavelength for y-polarized pump light. The inset shows the generated second harmonic power as a function of the azimuth of the linear pump polarization at 1510 nm pump wavelength (the resonance). Dots indicate measurements, and the blue curve shows a fit.

second harmonic above the noise level. The second harmonic nature of the signal is confirmed by its dependence on the average pump power at 1510 nm wavelength; see Fig. 2(b). The second harmonic spectral peak coincides with the metamaterial's absorption resonance, as expected from microscopic theory of second harmonic generation.[42]

2.9 pW second harmonic power (P_{SH}) has been observed for 35 mW y-polarized average pump power (P_{pump}), corresponding to a SHG power conversion efficiency of at least $\eta = P_{SH}/P_{pump} = 0.8 \times 10^{-10}$, which is comparable with efficiencies in metallic structures[43,44] and exceeds that of previously reported silicon metamaterial by four orders of magnitude.[28] We note that the fiber's refractive index of about 1.45 implies that some diffraction will occur into the fiber at free-space wavelengths shorter than 1.6 μm, while diffraction into air occurs at wavelengths shorter than 1.1 μm. The fiber's numerical aperture of 0.13 implies that only radiation propagating close to normal to the metamaterial will be collected. Therefore, the calculated efficiency of our structure only accounts for 0th order diffraction of SHG into the fiber. Diffraction of SHG up to the first order into air and up to the second order into glass implies that the metamaterial's true SHG efficiency may be a few times higher. To allow for comparison with other materials, we need to consider that phase-matched—sufficiently thin films are always phase-matched—SH conversion efficiency increases linearly with pump peak intensity I and quadratically with interaction length L. With $L = 346$ nm, we arrive at a normalized efficiency of $\eta/(IL^2) = 8 \times 10^{-3}$ GW^{-1} corresponding to $\chi_{yyy}^{(2)} \sim 0.3$ pm/V, which is comparable to KDP.[45] The normalized efficiency reported here exceeds that of previous silicon metamaterial[28] by two orders of magnitude. This improvement is largely due to resonant enhancement of second harmonic generation at the closed-mode resonance of the double-chevron structure.

According to symmetry analysis,[46] this metamaterial—and any other 2D structure of D_1 symmetry with symmetry axis y—has three

allowed components of the second-order susceptibility: $\chi_{yyy}^{(2)}$, $\chi_{yxx}^{(2)}$, and $\chi_{xyx}^{(2)} = \chi_{xxy}^{(2)}$. However, second harmonic detection through the standard single-mode fiber, which hosts the nonlinear metamaterial and does not maintain polarization, does not allow for direct polarization measurements on the generated second harmonic light. In order to probe the relative strengths of the allowed susceptibility tensor components, second harmonic power was detected with left-circularly, right-circularly, and linearly polarized pump light at several orientations relative to the metamaterial's symmetry axis. The inset in Fig. 2(b) shows generated second harmonic power as a function of the azimuth of the linear pump polarization at 1510 nm pump wavelength. The second-order susceptibility tensor components were extracted by fitting the pump-polarization-dependent intensity of the generated second harmonic signal, giving $\left|\chi_{xyx}^{(2)}/\chi_{yyy}^{(2)}\right| = 0.2$ and $\left|\chi_{yxx}^{(2)}/\chi_{yyy}^{(2)}\right| = 0.2$ at this resonant wavelength. $\chi_{yyy}^{(2)}$ is the dominant susceptibility tensor component. More details are provided in the supplementary material, Sec. S1.

Beyond symmetry considerations and the observed Fano resonance, we note that the structure may also support guided modes within the metamaterial layer,[47,48] which could play a role in coupling resonators and SHG. Furthermore, while diffraction above the 0th order will not be guided by the fiber and thus cannot contribute directly to the detected SHG, it could affect the conversion efficiency indirectly.

Our results show how pumping at an anti-symmetric Fano-type resonance of a structure lacking inversion symmetry yields substantial second harmonic generation in an amorphous silicon metamaterial. We believe that the second-order nonlinearity can be increased further by increasing the Q-factor of this resonance and by engineering a second resonance at the SHG wavelength. This may be achieved by adjusting the metamaterial design, more accurate nanofabrication (to avoid inhomogeneous broadening), and by avoiding gallium ion implantation during

nanofabrication (e.g., by using electron beam lithography or imprint techniques).

IV. CONCLUSIONS

In summary, we have demonstrated second harmonic generation in an amorphous silicon metamaterial with a power conversion efficiency of $\sim 10^{-10}$, an efficiency improvement of four orders of magnitude over previous silicon metamaterials. This improvement is achieved by exploiting the double-chevron structure's closed-mode resonance. Our findings demonstrate how mesoscopic structuring—that combines closed-mode resonances with a suitable choice of point group symmetry—enables the fabrication of metamaterials with quadratic optical nonlinearity from amorphous dielectrics. Second harmonic generation by the double-chevron metamaterial of D_1 symmetry is most efficient for pump light polarized along its symmetry axis, and all allowed net second-order nonlinear susceptibility tensor components have been determined. Ease of deposition of amorphous materials shall enable the fabrication of nonlinear elements of nanoscale thickness on complex non-planar platforms, such as end-facets of optical fibers and silicon photonics waveguides.

SUPPLEMENTARY MATERIAL

See the supplementary material for the complex refractive index of the silicon layer, the metamaterial's modeled electric field enhancement at the silicon interfaces, and the details of the nonlinear tensor characterization.

ACKNOWLEDGMENTS

DATA AVAILABILITY

The data that support the findings of this study are openly available in ePrints research repository, University of Southampton, at http://doi.org/10.5258/SOTON/D1626.

REFERENCES

[1] J. Butet, P.-F. Brevet, and O. J. F. Martin, "Optical second harmonic generation in plasmonic nanostructures: From fundamental principles to advanced applications," ACS Nano 9, 10545–10562 (2015).

[2] R. Czaplicki, A. Kiviniemi, M. J. Huttunen, X. Zang, T. Stolt, I. Vartiainen, J. Butet, M. Kuittinen, O. J. F. Martin, and M. Kauranen, "Less is more: Enhancement of second-harmonic generation from metasurfaces by reduced nanoparticle density," Nano Lett. 18, 7709–7714 (2018).

[3] S. D. Gennaro, M. Rahmani, V. Giannini, H. Aouani, T. P. H. Sidiropoulos, M. Navarro-Cía, S. A. Maier, and R. F. Oulton, "The interplay of symmetry and scattering phase in second harmonic generation from gold nanoantennas," Nano Lett. 16, 5278–5285 (2016).

[4] Y. B. Habibullah, K. Iwata, and T. Ishihara, "Second-harmonic generation from complementary Au metasurfaces with triangular resonators," J. Opt. Soc. Am. B 36, 1166–1175 (2019).

[5] J. Lee, M. Tymchenko, C. Argyropoulos, P.-Y. Chen, F. Lu, F. Demmerle, G. Boehm, M.-C. Amann, A. Alù, and M. A. Belkin, "Giant nonlinear response from plasmonic metasurfaces coupled to intersubband transitions," Nature 511, 65–69 (2014).

[6] N. Nookala, J. Lee, M. Tymchenko, J. S. Gomez-Diaz, F. Demmerle, G. Boehm, K. Lai, G. Shvets, M.-C. Amann, A. Alu, and M. Belkin, "Ultrathin gradient nonlinear metasurface with a giant nonlinear response," Optica 3, 283–288 (2016).

[7] N. C. Panoiu, W. E. I. Sha, D. Y. Lei, and G.-C. Li, "Nonlinear optics in plasmonic nanostructures," J. Opt. 20, 083001 (2018).

[8] T. Chang, S. Jeon, M. Heo, and J. Shin, "Mimicking bio-mechanical principles in photonic metamaterials for giant broadband nonlinearity," Commun. Phys. 3, 79 (2020).

[9] S. Liu, M. B. Sinclair, S. Saravi, G. A. Keeler, Y. Yang, J. Reno, G. M. Peake, F. Setzpfandt, I. Staude, T. Pertsch, and I. Brener, "Resonantly enhanced second-harmonic generation using III–V semiconductor all-dielectric metasurfaces," Nano Lett. 16, 5426–5432 (2016).

[10] F. J. F. Löchner, A. N. Fedotova, S. Liu, G. A. Keeler, G. M. Peake, S. Saravi, M. R. Shcherbakov, S. Burger, A. A. Fedyanin, I. Brener, T. Pertsch, F. Setzpfandt, and I. Staude, "Polarization-dependent second harmonic diffraction from resonant GaAs metasurfaces," ACS Photonics 5, 1786–1793 (2018).

[11] P. P. Vabishchevich, S. Liu, M. B. Sinclair, G. A. Keeler, G. M. Peake, and I. Brener, "Enhanced second-harmonic generation using broken symmetry III–V semiconductor Fano metasurfaces," ACS Photonics 5, 1685–1690 (2018).

[12] I. Volkovskaya, L. Xu, L. Huang, A. I. Smirnov, A. E. Miroshnichenko, and D. Smirnova, "Multipolar second-harmonic generation from high-Q quasi-BIC states in subwavelength resonators," Nanophotonics 9, 3953–3963 (2020).

[13] A. E. Minovich, A. E. Miroshnichenko, A. Y. Bykov, T. V. Murzina, D. N. Neshev, and Y. S. Kivshar, "Functional and nonlinear optical metasurfaces," Laser Photonics Rev. 9, 195–213 (2015).

[14] C. Langrock, S. Kumar, J. E. McGeehan, A. E. Willner, and M. M. Fejer, "All-optical signal processing using $\chi^{(2)}$ nonlinearities in guided-wave devices," J. Lightwave Technol. 24, 2579–2592 (2006).

[15] A. E. Willner, A. Fallahpour, F. Alishahi, Y. Cao, A. Mohajerin-Ariaei, A. Almaiman, P. Liao, K. Zou, A. N. Willner, and M. Tur, "All-optical signal processing techniques for flexible networks," J. Lightwave Technol. 37, 21–35 (2019).

[16] L. Alloatti, D. Korn, C. Weimann, C. Koos, W. Freude, and J. Leuthold, "Second-order nonlinear silicon-organic hybrid waveguides," Opt. Express 20, 20506–20515 (2012).

[17] I. Avrutsky and R. Soref, "Phase-matched sum frequency generation in strained silicon waveguides using their second-order nonlinear optical susceptibility," Opt. Express 19, 21707–21716 (2011).

[18] M. Cazzanelli, F. Bianco, E. Borga, G. Pucker, M. Ghulinyan, E. Degoli, E. Luppi, V. Véniard, S. Ossicini, D. Modotto, S. Wabnitz, R. Pierobon, and L. Pavesi, "Second-harmonic generation in silicon waveguides strained by silicon nitride," Nat. Mater. 11, 148–154 (2012).

[19] N. K. Hon, K. K. Tsia, D. R. Solli, and B. Jalali, "Periodically poled silicon," Appl. Phys. Lett. 94, 091116 (2009).

[20] R. S. Jacobsen, K. N. Andersen, P. I. Borel, J. Fage-Pedersen, L. H. Frandsen, O. Hansen, M. Kristensen, A. V. Lavrinenko, G. Moulin, H. Ou, C. Peucheret, B. Zsigri, and A. Bjarklev, "Strained silicon as a new electro-optic material," Nature 441, 199–202 (2006).

[21] A. Rao and S. Fathpour, "Second-harmonic generation in integrated photonics on silicon," Phys. Status Solidi A 215, 1700684 (2018).

[22] C. Castellan, A. Trenti, C. Vecchi, A. Marchesini, M. Mancinelli, M. Ghulinyan, G. Pucker, and L. Pavesi, "On the origin of second harmonic generation in silicon waveguides with silicon nitride cladding," Sci. Rep. 9, 1088 (2019).

[23] S. V. Makarov, M. I. Petrov, U. Zywietz, V. Milichko, D. Zuev, N. Lopanitsyna, A. Kuksin, I. Mukhin, G. Zograf, E. Ubyivovk, D. A. Smirnova, S. Starikov, B. N. Chichkov, and Y. S. Kivshar, "Efficient second-harmonic generation in nanocrystalline silicon nanoparticles," Nano Lett. 17, 3047–3053 (2017).

[24] M. Khorasaninejad, M. A. Swillam, K. Pillai, and S. S. Saini, "Silicon nanowire arrays with enhanced optical properties," Opt. Lett. 37, 4194–4196 (2012).

[25] P. R. Wiecha, A. Arbouet, H. Kallel, P. Periwal, T. Baron, and V. Paillard, "Enhanced nonlinear optical response from individual silicon nanowires," Phys. Rev. B 91, 121416 (2015).

[26] B. Dev Choudhury, P. K. Sahoo, R. Sanatinia, G. Andler, S. Anand, and M. Swillo, "Surface second harmonic generation from silicon pillar arrays with strong geometrical dependence," Opt. Lett. 40, 2072–2075 (2015).

[27] M. Galli, D. Gerace, K. Welna, T. F. Krauss, L. O'Faolain, G. Guizzetti, and L. C. Andreani, "Low-power continuous-wave generation of visible harmonics in silicon photonic crystal nanocavities," Opt. Express 18, 26613–26624 (2010).

[28] J. Bar-David and U. Levy, "Nonlinear diffraction in asymmetric dielectric metasurfaces," Nano Lett. 19, 1044–1051 (2019).

[29] Y. Q. An and A. C. Diebold, "Transiently stimulated second-harmonic generation from silicon nanogratings," Phys. Rev. B 96, 201306 (2017).

[30] K.-T. Lee, M. Taghinejad, J. Yan, A. S. Kim, L. Raju, D. K. Brown, and W. Cai, "Electrically biased silicon metasurfaces with magnetic Mie resonance for tunable harmonic generation of light," ACS Photonics 6, 2663–2670 (2019).

[31] H.-H. Lin, M.-H. Yang, R. Sharma, M. W. Puckett, S. Montoya, C. D. Wurm, F. Vallini, E. E. Fullerton, and Y. Fainman, "Synthesis of second-order nonlinearities in dielectric-semiconductor-dielectric metamaterials," Appl. Phys. Lett. 110, 113103 (2017).

[32] H.-H. Lin, F. Vallini, M.-H. Yang, R. Sharma, M. W. Puckett, S. Montoya, C. D. Wurm, E. E. Fullerton, and Y. Fainman, "Electronic metamaterials with tunable second-order optical nonlinearities," Sci. Rep. 7, 9983 (2017).

[33] N. Bernhardt, K. Koshelev, S. J. U. White, K. W. C. Meng, J. E. Fröch, S. Kim, T. T. Tran, D.-Y. Choi, Y. Kivshar, and A. S. Solntsev, "Quasi-BIC resonant enhancement of second-harmonic generation in WS$_2$ monolayers," Nano Lett. 20, 5309–5314 (2020).

[34] Q. Yuan, L. Fang, H. Fang, J. Li, T. Wang, W. Jie, J. Zhao, and X. Gan, "Second harmonic and sum-frequency generations from a silicon metasurface integrated with a two-dimensional material," ACS Photonics 6, 2252–2259 (2019).

[35] S. Bhagavantam and P. Chandrasekhar, "Harmonic generation and selection rules in nonlinear optics," Proc. - Indian Acad. Sci., Sect. A 76, 13–20 (1972).

[36] K. Konishi, T. Higuchi, J. Li, J. Larsson, S. Ishii, and M. Kuwata-Gonokami, "Polarization-controlled circular second-harmonic generation from metal hole arrays with threefold rotational symmetry," Phys. Rev. Lett. 112, 135502 (2014).

[37] V. A. Fedotov, M. Rose, S. L. Prosvirnin, N. Papasimakis, and N. I. Zheludev, "Sharp trapped-mode resonances in planar metamaterials with a broken structural symmetry," Phys. Rev. Lett. 99, 147401 (2007).

[38] B. Luk'yanchuk, N. I. Zheludev, S. A. Maier, N. J. Halas, P. Nordlander, H. Giessen, and C. T. Chong, "The Fano resonance in plasmonic nanostructures and metamaterials," Nat. Mater. 9, 707–715 (2010).

[39] S. Campione, S. Liu, L. I. Basilio, L. K. Warne, W. L. Langston, T. S. Luk, J. R. Wendt, J. L. Reno, G. A. Keeler, I. Brener, and M. B. Sinclair, "Broken symmetry dielectric resonators for high quality factor Fano metasurfaces," ACS Photonics 3, 2362–2367 (2016).

[40] V. Savinov and N. I. Zheludev, "High-quality metamaterial dispersive grating on the facet of an optical fiber," Appl. Phys. Lett. 111, 091106 (2017).

[41] N. Bloembergen, R. K. Chang, and C. H. Lee, "Second-harmonic generation of light in reflection from media with inversion symmetry," Phys. Rev. Lett. 16, 986–989 (1966).

[42] K. O'Brien, H. Suchowski, J. Rho, A. Salandrino, B. Kante, X. Yin, and X. Zhang, "Predicting nonlinear properties of metamaterials from the linear response," Nat. Mater. 14, 379–383 (2015).

[43] S. Keren-Zur, O. Avayu, L. Michaeli, and T. Ellenbogen, "Nonlinear beam shaping with plasmonic metasurfaces," ACS Photonics 3, 117–123 (2016).

[44] N. Segal, S. Keren-Zur, N. Hendler, and T. Ellenbogen, "Controlling light with metamaterial-based nonlinear photonic crystals," Nat. Photonics 9, 180–184 (2015).

[45] R. W. Boyd, Nonlinear Optics, 3rd ed. (Academic Press, Burlington, MA, 2008).

[46] S. Popov, Y. P. Svirko, and N. I. Zheludev, Susceptibility Tensors for Nonlinear Optics (CRC Press, 1995).

[47] M. Gould, A. Pomerene, C. Hill, S. Ocheltree, Y. Zhang, T. Baehr-Jones, and M. Hochberg, "Ultra-thin silicon-on-insulator strip waveguides and mode couplers," Appl. Phys. Lett. 101, 221106 (2012).

[48] Z. Zou, L. Zhou, X. Li, and J. Chen, "60-nm-thick basic photonic components and Bragg gratings on the silicon-on-insulator platform," Opt. Express 23, 20784–20795 (2015).